Chapter 5

Performance Analysis of the Differential Evolution and Particle Swarm Optimization Algorithms in Cooperative Wireless Communications

Arif Basgumus, Mustafa Namdar, Gunes Yilmaz and Ahmet Altuncu

Additional information is available at the end of the chapter

http://dx.doi.org/10.5772/62453

Abstract

In this study, we evaluate the performance of differential evolution (DE) and particle swarm optimization (PSO) algorithms in free-space optical (FSO) and mobile radio communications systems. In particular, we obtain the optimal transmission distances for multiple-relay nodes in FSO communication systems and optimal relay locations in mobile radio communications systems for the cooperative-diversity networks, using both algorithms. We investigate the performance comparison of DE and PSO algorithms for the parallel decode-and-forward (DF) relaying. Then, we analyze the cost functions. Furthermore, we present the execution time and the stability of the DE and PSO algorithms.

Keywords: free-space optical communications, cooperative-diversity networks, optimal distance, differential evolution algorithm, particle swarm optimization algorithm

1. Introduction

The aim of the optimization was to provide the best-suited solution to a problem under the given constraints. The optimization algorithms have recently been much attention and gained significant importance in plenty of engineering problems [1–8]. In this study, we evaluate the performance analysis of differential evolution (DE) and particle swarm optimization (PSO) algorithms both in free-space optical (FSO) and in mobile radio communications systems.

INTECH
open science | open minds

© 2016 The Author(s). Licensee InTech. This chapter is distributed under the terms of the Creative Commons Attribution License (http://creativecommons.org/licenses/by/3.0), which permits unrestricted use, distribution, and reproduction in any medium, provided the original work is properly cited.

FSO communications have been proposed as a solution for the various applications including fiber backup, and backhaul for wireless communications networks [9]. Despite the fact that the usage of FSO communications is widespread in major applications for wireless communications, the performance limitations for long-range links due to the atmospheric turbulence-induced fading have had profound impacts in FSO communications systems. The method used for relay-assisted FSO transmission links is one of the fading mitigation technique has attracted significant attentions recently in FSO communications networks [9–11]. In [9], the authors consider relay-assisted FSO communications and investigate the outage performance under serial and parallel scheme with amplify-and-forward (AF), and decode-and-forward (DF) relaying models. The authors in [10] consider a cooperative FSO communications via optical AF relay and investigate the bit error probability performance. Bit error rate (BER) analysis of cooperative systems in FSO networks is presented in [11]. The outage performance analysis of FSO communications is presented in both [12] and [13]. Kashani et al. [14] consider the diversity gain analysis and determine the optimal relay locations for both the serial and the parallel relaying schemes. Although cooperative transmissions have greatly been considered in the above manuscripts, to the best of the authors' knowledge, there has not been any notable research for the relay-assisted FSO communications systems using the optimization algorithms. To fill the research gap, in this paper, we analyze the performance of both DE and PSO algorithms in terms of the transmission distances when applied for the parallel DF relaying in FSO systems. Moreover, we investigate the performance comparison of these two algorithms in respect to the execution time, cost, and stability analysis.

In our study, as a second part of this paper, we focus on dual-hop cooperative-diversity network to study the impact of the relay location between the source and the destination. Cooperative-diversity relay networks provide a significant performance increment in the radio frequency power transmission and the spatial diversity. They are also shown to be a promising solution to mitigate the signal fading arising from the multipath propagation in wireless communications [15, 16]. In the cooperative-diversity networks, relay terminals are employed between the transmitter and receiver nodes, over multiple communications routes, in which two main protocols are used as follows: (i) amplify-and-forward and (ii) DF [15–21].

Most of the previous publications have studied the cooperative-diversity performance over different fading channels [15–26]. In [15], the authors analyzed the cooperative-diversity network using AF cooperation protocol, operating over independent, but not necessarily identically distributed Nakagami-m fading channels. The paper in [17] addressed the multi-branch adaptive DF scheme for cooperative-diversity networks. The best relay selection scheme for cooperative-diversity network is studied in [18]. Furthermore, [19] investigated the advantage of the diversity over direct transmission and conventional non-cooperative relaying scheme. In all these papers, analytical framework for performance analysis of BER and the outage probability is provided [15, 17–19]. As far as we know, both DE and PSO algorithms have not been applied for obtaining the optimal location of the relaying terminal over Nakagami-m fading channel.

To fill the research gaps in mobile radio communications using cooperative-diversity relay network, in this paper, we provide an optimization algorithms results, indicating the optimal location of the relaying terminal in the parallel-relaying scheme.

In summary, for the first part of this paper, the key contributions are twofold:

- First, the locations of each individual relay nodes and the transmission distances are optimized for the parallel DF relaying scheme in FSO systems.
- Second, and more importantly, none of the previous studies provide a comparison among optimization algorithms when applied for FSO systems. In this paper, we investigate the performance comparison of DE and PSO algorithms for the parallel DF relaying in respect to the execution time, cost, and stability analysis.

For the second part of this paper, there is a major contribution:

- To fill the research gaps in cooperative-diversity relay network, we provide a rigorous data for the optimal location of the relaying terminal over Nakagami-m fading channel achieving the best error performance using both DE and PSO algorithms in the parallel relaying schemes.

The rest of this paper is organized as follows: The system model and performance analysis are discussed in Section 2 exploiting the DE and PSO algorithms. Section 3 provides the numerical results and simulations. Finally, the concluding remarks are given in Section 4.

2. System model and performance analysis using the optimization algorithms

2.1. FSO communications systems

This section presents the system model for FSO communications networks with parallel DF cooperative relaying protocol shown in **Figure 1a**. We consider that the FSO links between the source-to-relay ($S \rightarrow R_j$, $j = 1, 2, \ldots, M$) and relay-to-destination ($R_j \rightarrow D$) are subjected to atmospheric turbulence-induced log-normal fading [1]. Here, the j index refers to the number of the relay nodes, where the maximum number of relay nodes (R_j) is defined with M ($j = 1, 2, \ldots, M$) as shown in **Figure 1a**. Besides, the normalized path loss can be expressed as $L(d) = \frac{\ell(d)}{\ell(d_{S,D})} = \left(\frac{d_{S,D}}{d}\right)^2 e^{\sigma(d_{S,D}-d)}$ where $\ell(d)$ and $\ell(d_{S,D})$ are defined as the path losses for the distance of d and for the distance between source and destination ($d_{S,D}$), respectively [13, 14]. Here, σ is the atmospheric attenuation coefficient. In the same figure below, d_{S,R_j} is the distance between the source and the $j-th$ decoding relay, and $d_{R_j,D}$ is the direct link distance between the $j-th$ relay and the destination where the relay nodes are placed on the straight line connecting the source and the destination.

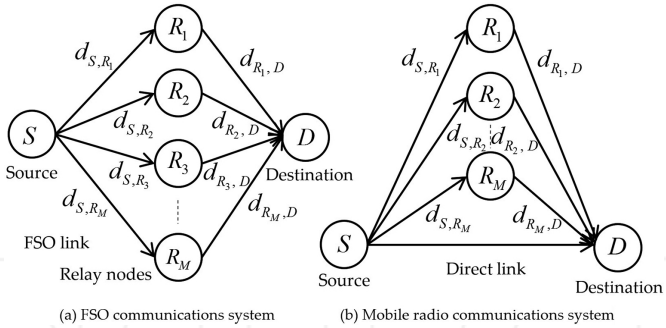

Figure 1. System models for cooperative wireless communications.

In [14], the outage probability for the parallel DF relaying is expressed as follows:

$$P_{out} = \sum_{i=1}^{2^M} \left[\prod_{j \in W(i)} \left(1 - Q\left(\frac{\ln\left(\frac{L\left(d_{S,R_j}\right)P}{2M} \right) + 2\mu_\chi\left(d_{S,R_j}\right)}{2\sigma_\chi\left(d_{S,R_j}\right)} \right) \right) \right.$$
$$\left. \times \prod_{j \notin W(i)} Q\left(\frac{\ln\left(\frac{L\left(d_{S,R_j}\right)P}{2M} \right) + 2\mu_\chi\left(d_{S,R_j}\right)}{2\sigma_\chi\left(d_{S,R_j}\right)} \right) \right] Q\left(\frac{\ln\left(\frac{Pe^{\mu_\xi}}{2M} \right)}{\sigma_\xi\left(\bar{d}_{W(i)}\right)} \right) \tag{1}$$

where $Q(x) = \frac{1}{\sqrt{2\pi}} \int_x^\infty \exp\left(-\frac{u^2}{2}\right) du$ is the Q function, M is the relay number. Here, P is the power margin and defined by $P = (P_T/P_{th})$, where P_T is the total transmitted power, and P_{th} is the threshold value for the transmit power in case of no outage is available. P_T is expressed as $P_T = P_S + \sum_{j=1}^{M} P_j$, where P_S is the source power, and P_j is the power of the $j - th$ relay [9]. In Eq. (1), the variance of the fading log-amplitude, χ is defined by $\sigma_\chi^2(d) = min\ \{0.124\ k^{(7/6)}\ C_n^2\ d^{(11/6)}, 0.5\}$, where $k = (2\pi/\lambda)$ is the wave number, and $C_n^2 = 10^{-14} m^{2/3}$ is the refractive index structure constant [14]. Here, ln(.) is the natural logarithm operator and λ is the wavelength [10]. The mean value of the fading log-amplitude is modeled as $\mu_\chi = -\sigma_\chi^2$ [11].

In the outage probability of the parallel DF relaying scheme, there are 2^M possibilities for decoding the signal between S and R_j. In Eq. (1) the i index refers to the number of possible

http://dx.doi.org/10.5772/62453

combinations where the $i-th$ possible set is defined by $W(i)$, and the possible set of distances between the relays and destination is given by $\bar{d}_{W(i)}$. μ_ξ is the mean value, and σ_ξ is the variance of the log-amplitude factor, also given in [9, 14].

For the optimization problem, a function is employed to minimize the outage probability for the parallel DF relaying, which can be written as $\min\{P_{out}\}=\min\{f(d_{S,R_1}, d_{S,R_2}, \ldots, d_{S,R_M})\}$ where $0<d_{S,R_j}<d_{S,D}$ for $j = 1, 2,...., M$. Optimal transmission distance is maximized by optimizing the locations of the relays, at an outage probability of 10^{-6} as modeled as follows [27]:

$$\max\{d_{S,D}\} = f\left(\min\left\{\left|\min\{P_{out}\} - 10^{-6}\right|\right\}\right) \tag{2}$$

The flowcharts for the optimization of the transmission distance using DE and PSO algorithms are shown in **Figures 2** and **3**, successively.

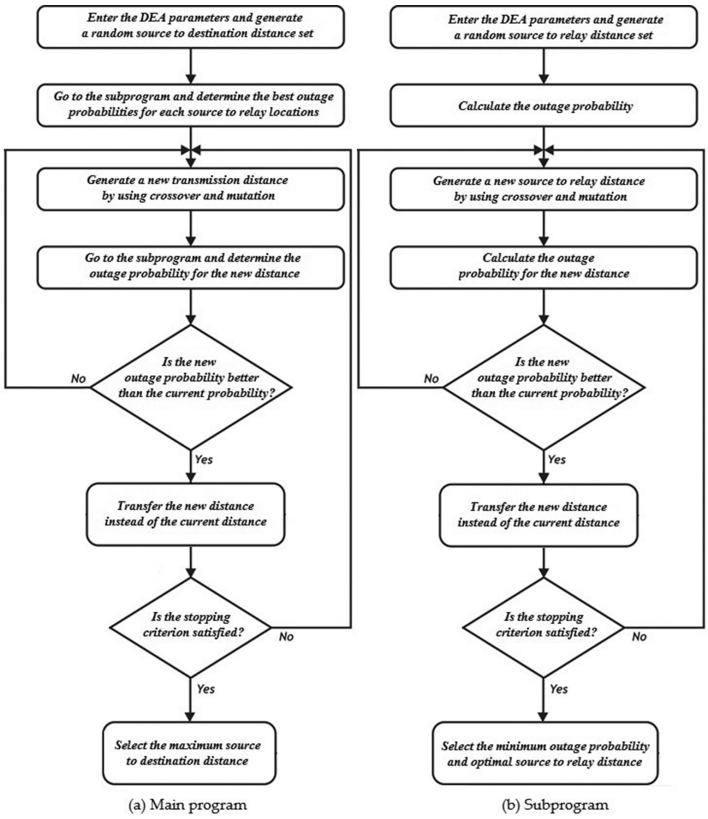

Figure 2. The flowcharts for the optimization of the transmission distance by using DE algorithm.

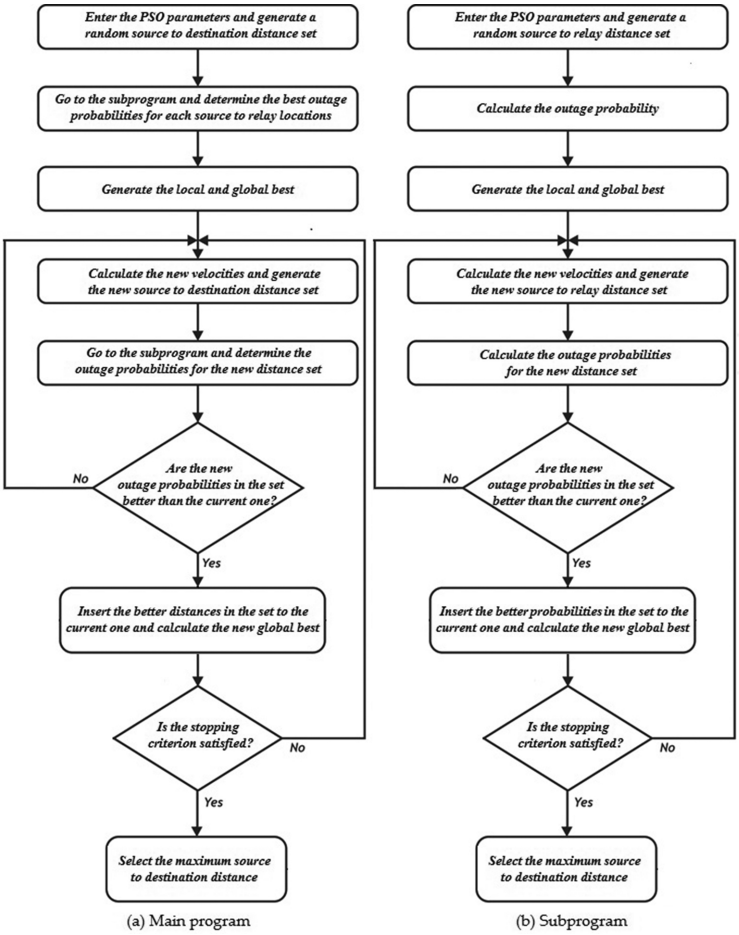

Figure 3. The flowcharts for the optimization of the transmission distance by using PSO algorithm.

2.2. Mobile radio communications systems using cooperative-diversity relay networks

A system, consisting of a source terminal (S), a cooperative relay terminal (R_j, $j = 1, 2, \ldots, M$), and a destination terminal (D), is considered, as shown in **Figure 1b**. The source and the destination operate in half-duplex mode and both equipped with a single pair of transmit and receive antennas. Source communicates with the destination over both the direct link and relaying terminal links [17, 20]. The cooperation method is based on DF relaying in which the source information is decoded first and then retransmitted to the destination. We consider that the received signals from the source and the relays are combined together using the method of equal gain combining (EGC) [15, 17, 28]. We assume that the diversity paths between the source-to-relay terminals ($S \rightarrow R_j$) and the relay terminals-to-destination ($R_j \rightarrow D$) are

independent non-identically distributed Nakagami-m fading. The direct link between the source and destination ($S \rightarrow D$) has also Nakagami-m distribution. Besides, the additive white Gaussian noise (AWGN) terms of $S \rightarrow D$ link, $S \rightarrow R_j$ and $R_j \rightarrow D$ links have zero mean and equal variance of N_0 [15, 17].

The source signal is transmitted with the energy of E_s, directly to the destination D, and the relays. The relays decode and transmit the multiple copies of the original source signal to the destination. Finally, at the destination, the direct and indirect links from the source and the relays are combined together. It should be noted that, at the destination, the total output signal-to-noise ratio (SNR) can be expressed as [15, 17]

$$\gamma_{Total} = \gamma_{SD} + \sum_{i=1}^{M} \frac{\gamma_{S,R_j}\gamma_{R_j,D}}{\gamma_{S,R_j} + \gamma_{R_j,D} + 1} \tag{3}$$

where $\gamma_{SD} = \frac{E_s}{N_0} h_{SD}^2$, $\gamma_{S,R_j} = \frac{E_s}{N_0} h_{S,R_j}^2$, and $\gamma_{R_j,D} = \frac{E_s}{N_0} h_{R_j,D}^2$ are the instantaneous SNRs, in the $S \rightarrow D$ link, between S and the $j-th$ relay, and between the relay, R_j and the destination, successively [13, 14]. Note that, $h_{S,D}$, h_{S,R_j}, and $h_{R_j,D}$ represent the channel fading coefficients for $S \rightarrow D$, $S \rightarrow R_j$, and $R_j \rightarrow D$ links, respectively [13]. Finally, a closed form for the error performance of the DF scheme for the cooperative-diversity relay network is given in [14] as follows:

$$\begin{aligned} P(e) \le & \frac{1}{2^{2M+1}} \sum_{i=1}^{M+1} \frac{(2M+1)!}{(M+1-i)!(M+i)!} \\ & \times \left[\left(\frac{3}{2} + \frac{1-\beta^{i-1}}{\pi\beta^{i-1}(1-\beta)} \right) M_{\gamma_{S,D}}(\varsigma) \prod_{k=1}^{M} M_i(\varsigma) - \left(\frac{1}{2} + \frac{1-\beta^{i-1}}{\pi\beta^{i-1}(1-\beta)} \right) M_{\gamma_{S,D}}(v) \prod_{k=1}^{M} M_i(v) \right] \end{aligned} \tag{4}$$

where $\beta = (a/b)$, $\varsigma = (b-a)^2/2$, $\upsilon = (b+a)^2/2$. In here, a and b are constant values depend on the modulation type. For instance, for differential binary phase shift keying (DBPSK) modulation $a = 10^{-3}$ and $b = \sqrt{2}$ [17]. $M_{\gamma_{S,D}}(\varsigma) = (1 + \varsigma(\bar{\gamma}_{S,D}/m_{S,D}))^{-m_{S,D}}$ is the moment-generating function (MGF) of $\gamma_{S,D}$, where $m_{S,D}$ is the fading parameter between the source and destination. In Eq. (4), $M_i(\varsigma) = A_i + (1-A_i) M_{\gamma_{R_i D}}(\varsigma)$ is the MGF of the $j-th$ indirect relay link variable ς where $M_{\gamma_{R_i D}}(\varsigma)$ is the MGF of $\gamma_{R_j,D}$, and expressed as $M_{\gamma_{R_i D}}(\varsigma) = \left(1 + \varsigma(\bar{\gamma}_{R_i D}/m_{R_i,D})\right)^{-m_{R_i,D}}$ [15]. Here, $m_{R_j,D}$ is the fading parameter between the $j-th$ relay and the destination and A_i can be given for DBPSK modulation as $A_i = \frac{1}{2}\left(m_{S,R_i}/\left(m_{S,R_i} + \bar{\gamma}_{S,R_i}\right)\right)^{m_{S R_i}}$ [17]. The average SNRs between S and D, S and the $j-th$ relay, and $j-th$ relay and the destination are denoted by $\bar{\gamma}_{S,D} = (E_s/N_0)$, $\bar{\gamma}_{S,R_i} = \left(d_{S,D}/d_{S,R_i}\right)^{\in}(E_s/N_0)$, and $\bar{\gamma}_{R_i,D} = \left(d_{S,D}/d_{R_i,D}\right)^{\in}(E_s/N_0)$, respectively, where $\in$ is the path loss exponent. The same approach in [15, 29, 30] is applied with the following model, while evaluating the effect of the path loss on the error performance: $\bar{h}_{S,R_j}^2 = E\left(h_{S,R_j}^2\right) = \left(\frac{d_{S,D}}{d_{S,R_j}}\right)^{\in}$,

$\bar{h}^2_{R_j,D} = E\left(h^2_{R_j,D}\right) = \left(\frac{d_{S,D}}{d_{R_j,D}}\right)^{\in}$, and $\bar{h}^2_{S,D} = \left(\frac{d_{S,D}}{d_{S,D}}\right)^{\in}$. Here, $E(.)$ is the statistical average operator, $d_{x,y}$ is the distance, and $\bar{h}^2_{x,y}$ is the average channel fading coefficient between the terminals x and y.

3. Numerical results and simulations

In this section, numerical and simulation results are presented for both FSO and mobile radio communication systems.

3.1. FSO communications systems

In this section, numerical results are presented. For the optimization algorithms, the parameters $\lambda = 1550\ nm$, $C_n^2 = 10^{-14} m^{2/3}$, $\sigma = 0.1$, $P = 9$ dB are used, and totally 4 relays are evaluated. The cost function analysis is illustrated in **Figure 4**, for the DE and PSO algorithms in terms of the iteration number. It can be observed from the simulation results that the cost function for the PSO algorithm is minimized for the small number of iterations as compare to the DE algorithm. This result indicates that PSO outperforms DE in terms of the cost function. Here, the iteration number is set to 40, and the execution number is taken as 50.

Figure 5 shows the optimal $d_{S,D}$ for the aforementioned algorithms. While 4 relays are used, $d_{S,D}$ = 6.0547 km is calculated. For the each execution, PSO algorithm gives almost the same result. Therefore, it is obvious that PSO is more stable than the DE algorithm under the same setup.

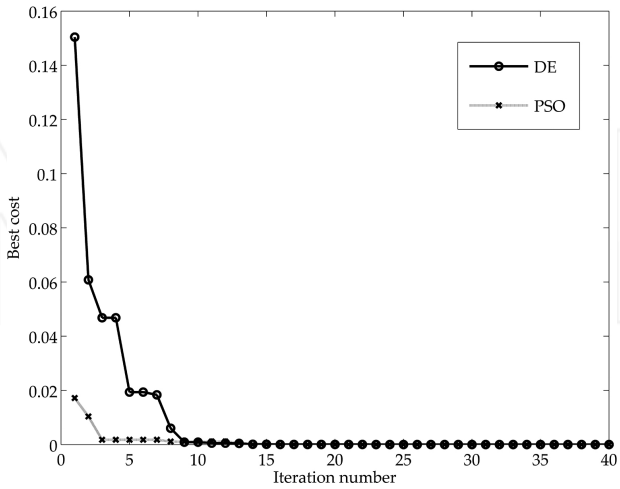

Figure 4. Cost function for 40 iterations.

http://dx.doi.org/10.5772/62453

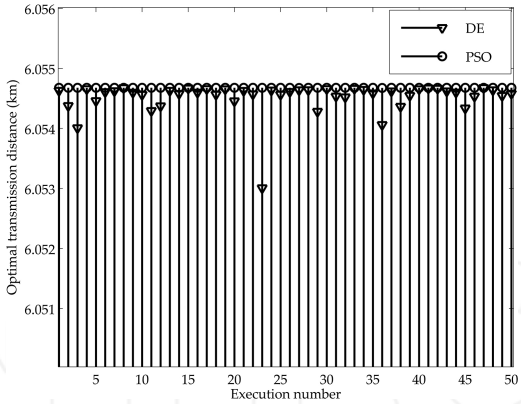

Figure 5. Optimal $d_{S,D}$ vs. execution number for the DE and PSO algorithms.

It can be noticed from **Figure 6** that the execution time for the PSO algorithm closely matches with the execution time of the DE algorithm for different number of relays.

Figure 7 shows the optimization results for the locations of each individual relay nodes. Accurate relay placements are obtained for $P = 9$ dB and 4 relays (R_j, $j = 1, 2, 3, 4$). The optimization results indicate that if the places of each individual relay nodes are similar, regardless of the relay number and the P value, better performance is achieved. **Figure 7** clearly shows that the optimal places of the relay nodes for both algorithms are calculated as $d_{S,R_j} \approx 0.4305$ using the normalized approach, after the number of iterations, which confirms the accuracy of the employed optimization algorithms. In addition, these results show that both algorithms seem to be the better optimization algorithms in providing the reliable and the rapid results.

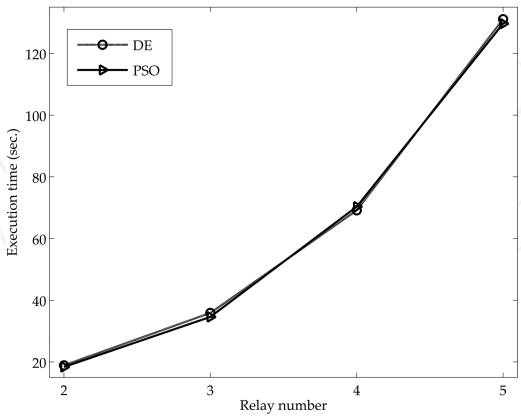

Figure 6. Execution time vs. relay number for the DE and PSO algorithms.

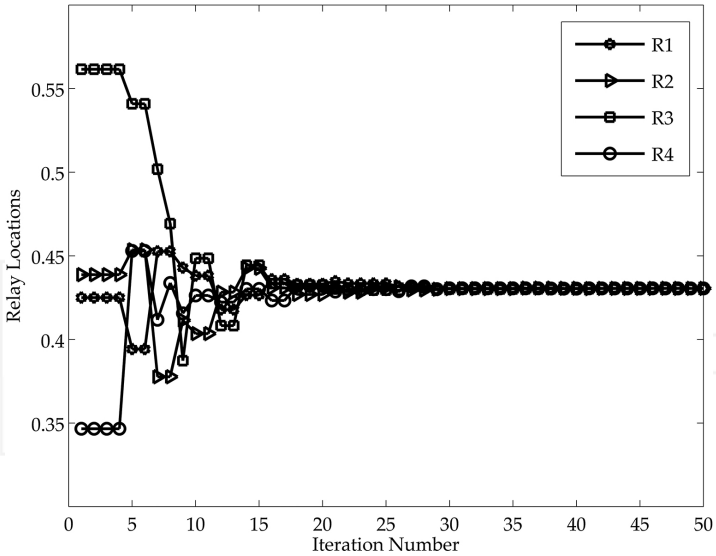

Figure 7. Relay location vs. iteration number for R_j, $j = 1,.., 4$.

Finally, the impact of the varying P on the optimal transmission distance for the DE and PSO algorithms is depicted in **Figure 8**. It can be seen from the below figure that the optimal

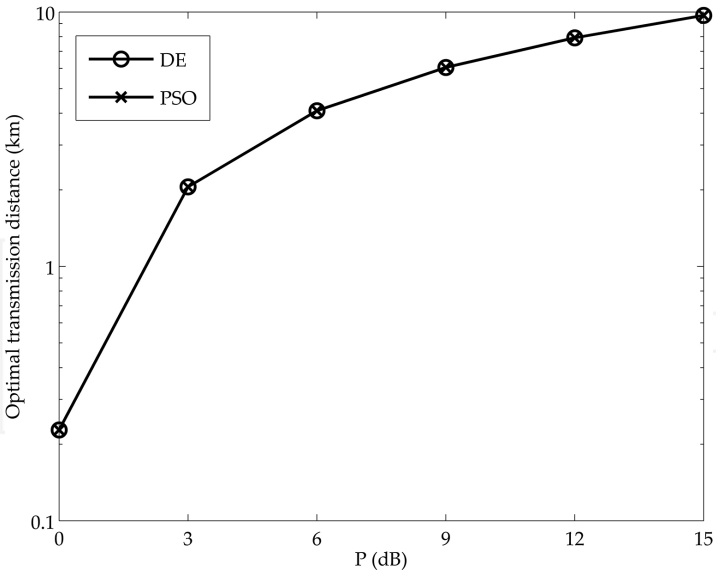

Figure 8. Optimal $d_{S,D}$ with varying P.

transmission distance increases with P and the results for both algorithms closely match with each other for all P values.

The detailed optimization results with the DE and PSO algorithms for DF parallel relaying scheme are given in **Table 1**. Here, the results for the optimal transmission distances and optimal relay locations are listed for various P values, where $d_{S,D}$ is the distance between the source and the destination ($S \rightarrow D$) and d_{S,R_j} is the distance between the source and the $j-th$ relay ($S \rightarrow R_j$, j = 1, 2, …, M). Based on the numerical optimization results provided in **Table 1**, while the number of relays is increased, the relays are obliged to get close up to the source, and the distance between the source and the destination is shortened in low P region, as expected [31].

P (dB)	2 Relays				3 Relays			
	DE		PSO		DE		PSO	
	Optimal $d_{S,D}$ (km)	Optimal d_{S,R_j} (km)	Optimal $d_{S,D}$ (km)	Optimal d_{S,R_j} (km)	Optimal $d_{S,D}$ (km)	Optimal d_{S,R_j} (km)	Optimal $d_{S,D}$ (km)	Optimal d_{S,R_j} (km)
0	0.6323	0.2608	0.6323	0.2608	0.4017	0.1464	0.4016	0.1463
3	2.0304	0.8562	2.0304	0.8562	2.0453	0.7813	2.0453	0.7813
6	3.5568	1.5653	3.5568	1.5653	3.8708	1.6044	3.8708	1.6044
9	5.1021	2.3490	5.1021	2.3490	5.6697	2.5207	5.6697	2.5207
12	6.6391	3.1868	6.6392	3.1868	7.4014	3.4801	7.4014	3.4801
15	8.1326	4.0077	8.1326	4.0077	9.0656	4.4476	9.0656	4.4476
P (dB)	4 Relays				5 Relays			
0	0.2276	0.0756	0.2276	0.0756	0.2276	0.0756	0.2276	0.0756
3	2.0541	0.7280	2.0541	0.7280	2.0541	0.7280	2.0541	0.7280
6	4.0930	1.6114	4.0930	1.6114	4.0930	1.6114	4.0930	1.6114
9	6.0547	2.6065	6.0547	2.6065	6.0547	2.6065	6.0547	2.6065
12	7.9173	3.6665	7.9173	3.6665	7.9173	3.6665	7.9173	3.6665
15	9.6952	4.7477	9.6952	4.7477	9.6952	4.7477	9.6952	4.7477

Table 1. Optimization results for the parallel DF relaying with different number of nodes.

3.2. Mobile radio communications systems

The error performance of the DF scheme for the cooperative-diversity relay network is illustrated in **Table 2** with varying path loss exponent for different values of E_s/N_0 when $m_{S,D}=m_{S,R_j}=m_{R_j,D}=1$, $\bar{h}^2_{S,D}=1$, and the number of relay is M = 1. The optimal relay placement ($d_{S,R}$) values to minimize the total error rate where the best minimum of $P(e)$ is achieved for the proposed system are calculated with the help of DE and PSO algorithms.

$\frac{E_s}{N_0}$	$\epsilon = 3$		$\epsilon = 4$		$\epsilon = 5$	
	Best BER	**Optimal $d_{S,R}$**	**Best BER**	**Optimal $d_{S,R}$**	**Best BER**	**Optimal $d_{S,R}$**
0	1.2993×10^{-1}	0.7518	8.8041×10^{-2}	0.6179	5.1268×10^{-2}	0.5721
1	1.0951×10^{-1}	0.7211	7.0389×10^{-2}	0.6083	3.9879×10^{-2}	0.5690
2	8.9635×10^{-2}	0.6962	5.5120×10^{-2}	0.6011	3.0535×10^{-2}	0.5667
3	7.1352×10^{-2}	0.6768	4.2307×10^{-2}	0.5956	2.3011×10^{-2}	0.5648
4	5.5332×10^{-2}	0.6621	3.1845×10^{-2}	0.5914	1.7065×10^{-2}	0.5632
5	4.1869×10^{-2}	0.6509	2.3521×10^{-2}	0.5881	1.2453×10^{-2}	0.5620
6	3.0965×10^{-2}	0.6424	1.7057×10^{-2}	0.5855	8.9429×10^{-3}	0.5610
7	2.2419×10^{-2}	0.6358	1.2155×10^{-2}	0.5834	6.3230×10^{-3}	0.5602
8	1.5917×10^{-2}	0.6307	8.5199×10^{-3}	0.5818	4.4044×10^{-3}	0.5595
9	1.1103×10^{-2}	0.6267	5.8820×10^{-3}	0.5805	3.0255×10^{-3}	0.5590
10	7.6227×10^{-3}	0.6236	4.0051×10^{-3}	0.5795	2.0518×10^{-3}	0.5585
11	5.1610×10^{-3}	0.6212	2.6938×10^{-3}	0.5786	1.3756×10^{-3}	0.5582
12	3.4523×10^{-3}	0.6193	1.7924×10^{-3}	0.5780	9.1298×10^{-4}	0.5579
13	2.2854×10^{-3}	0.6177	1.1816×10^{-3}	0.5774	6.0063×10^{-4}	0.5576
14	1.4998×10^{-3}	0.6165	7.7281×10^{-4}	0.5770	3.9220×10^{-4}	0.5575
15	9.7704×10^{-4}	0.6156	5.0210×10^{-4}	0.5767	2.5448×10^{-4}	0.5573
16	6.3264×10^{-4}	0.6148	3.2442×10^{-4}	0.5764	1.6426×10^{-4}	0.5572
17	4.0759×10^{-4}	0.6142	2.0866×10^{-4}	0.5762	1.0556×10^{-4}	0.5571
18	2.6153×10^{-4}	0.6138	1.3370×10^{-4}	0.5760	6.7596×10^{-5}	0.5570
19	1.6725×10^{-4}	0.6134	8.5414×10^{-5}	0.5759	4.3161×10^{-5}	0.5569
20	1.0668×10^{-4}	0.6131	5.4431×10^{-5}	0.5757	2.7493×10^{-5}	0.5569
21	6.7892×10^{-5}	0.6128	3.4618×10^{-5}	0.5757	1.7480×10^{-5}	0.5568
22	4.3133×10^{-5}	0.6126	2.1982×10^{-5}	0.5756	1.1097×10^{-5}	0.5568
23	2.7365×10^{-5}	0.6125	1.3940×10^{-5}	0.5755	7.0356×10^{-6}	0.5568
24	1.7342×10^{-5}	0.6124	8.8312×10^{-6}	0.5755	4.4564×10^{-6}	0.5568
25	1.0981×10^{-5}	0.6123	5.5901×10^{-6}	0.5755	2.8205×10^{-6}	0.5567

Table 2. Optimization results using the normalized approach for the parallel DF relaying with different path loss exponent for $m_{S,D}=m_{S,R_j}=m_{R_j,D}=1$, $\bar{h}^2_{S,D}=1$.

Figure 9 shows the best BER performance for the considered system versus E_s/N_0 when $m_{S,D}=m_{S,R_j}=m_{R_j,D}=1$, $\bar{h}^2_{S,D}=1$, and $M = 1$. The results clearly show that BER significantly decreases with the increase E_s/N_0. In the same figure, the path loss exponent ($\in$) is varied from 3 to 5.

http://dx.doi.org/10.5772/62453

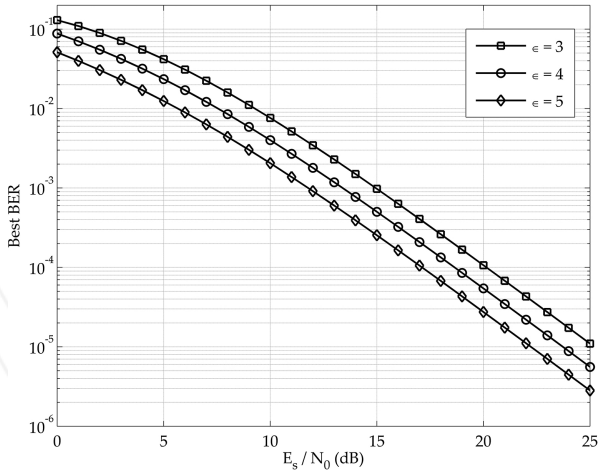

Figure 9. BER performance of the DF scheme for the cooperative-diversity relay network with ∈ = 3, 4, 5 and $m_{S,D}=m_{S,R_j}=m_{R_j,D}=1$.

Figure 10 demonstrates the effect of ∈ on the distance between source and the relay terminal ($d_{S,R}$) with varying E_s/N_0. This figure is plotted for $m_{S,D}=m_{S,R_j}=m_{R_j,D}=1$, and $\bar{h}^2_{S,D}=1$.

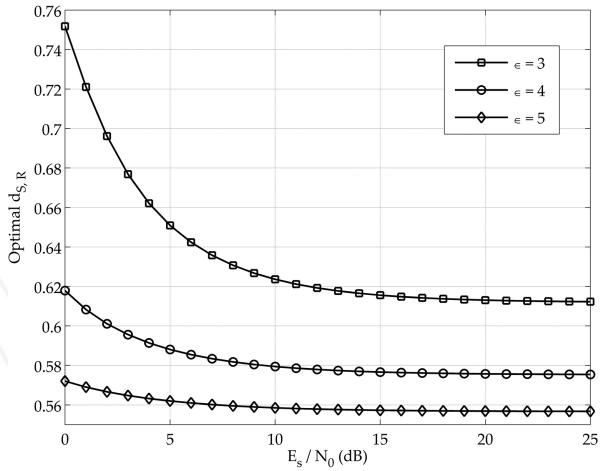

Figure 10. Optimal $d_{S,R}$ against different E_s/N_0 values with ∈ = 3, 4, 5 and $m_{S,D}=m_{S,R_j}=m_{R_j,D}=1$.

Table 3 shows that, the optimal $d_{S,R}$ can be calculated where the best minimum of $P(e)$ is achieved with varying E_s/N_0 for different values of ∈ when $m_{S,D}=m_{S,R_j}=m_{R_j,D}=2$, $\bar{h}^2_{S,D}=1$, and the number of relay is $M = 1$.

$\frac{E_s}{N_0}$	$\epsilon = 3$		$\epsilon = 4$		$\epsilon = 5$	
	Best BER	**Optimal $d_{S,R}$**	**Best BER**	**Optimal $d_{S,R}$**	**Best BER**	**Optimal $d_{S,R}$**
0	9.7528×10^{-2}	0.6525	4.6132×10^{-2}	0.5676	1.6573×10^{-2}	0.5409
1	7.4048×10^{-2}	0.6277	3.1667×10^{-2}	0.5610	1.0673×10^{-2}	0.5388
2	5.3487×10^{-2}	0.6091	2.0935×10^{-2}	0.5559	6.6843×10^{-3}	0.5370
3	3.6808×10^{-2}	0.5955	1.3343×10^{-2}	0.5521	4.0720×10^{-3}	0.5356
4	2.4167×10^{-2}	0.5855	8.2058×10^{-3}	0.5491	2.4121×10^{-3}	0.5345
5	1.5160×10^{-2}	0.5779	4.8710×10^{-3}	0.5468	1.3884×10^{-3}	0.5335
6	9.0972×10^{-3}	0.5722	2.7915×10^{-3}	0.5449	7.7597×10^{-4}	0.5327
7	5.2296×10^{-3}	0.5678	1.5448×10^{-3}	0.5433	4.2078×10^{-4}	0.5320
8	2.8842×10^{-3}	0.5644	8.2583×10^{-4}	0.5421	2.2129×10^{-4}	0.5314
9	1.5289×10^{-3}	0.5617	4.2681×10^{-4}	0.5410	1.1287×10^{-4}	0.5309
10	7.8074×10^{-4}	0.5595	2.1352×10^{-4}	0.5402	5.5873×10^{-5}	0.5305
11	3.8507×10^{-4}	0.5578	1.0358×10^{-4}	0.5395	2.6877×10^{-5}	0.5301
12	1.8397×10^{-4}	0.5564	4.8835×10^{-5}	0.5389	1.2586×10^{-5}	0.5298
13	8.5421×10^{-5}	0.5553	2.2434×10^{-5}	0.5385	5.7510×10^{-6}	0.5295
14	3.8672×10^{-5}	0.5545	1.0070×10^{-5}	0.5381	2.5705×10^{-6}	0.5293
15	1.7127×10^{-5}	0.5538	4.4297×10^{-6}	0.5378	1.1268×10^{-6}	0.5291
16	7.4433×10^{-6}	0.5532	1.9148×10^{-6}	0.5375	4.8576×10^{-7}	0.5290
17	3.1836×10^{-6}	0.5528	8.1544×10^{-7}	0.5373	2.0643×10^{-7}	0.5289
18	1.3436×10^{-6}	0.5524	3.4296×10^{-7}	0.5371	8.6671×10^{-8}	0.5288
19	5.6080×10^{-7}	0.5521	1.4276×10^{-7}	0.5370	3.6027×10^{-8}	0.5287
20	2.3194×10^{-7}	0.5519	5.8914×10^{-8}	0.5369	1.4852×10^{-8}	0.5286
21	9.5217×10^{-8}	0.5517	2.4143×10^{-8}	0.5368	6.0812×10^{-9}	0.5286
22	3.8852×10^{-8}	0.5516	9.8379×10^{-9}	0.5368	2.4762×10^{-9}	0.5286
23	1.5775×10^{-8}	0.5514	3.9902×10^{-9}	0.5367	1.0038×10^{-9}	0.5285
24	6.3802×10^{-9}	0.5513	1.6124×10^{-9}	0.5367	4.0545×10^{-10}	0.5285
25	2.5722×10^{-9}	0.5513	6.4960×10^{-10}	0.5366	1.6329×10^{-10}	0.5285

Table 3. Optimization results using the normalized approach for the parallel DF relaying with different path loss exponent for $m_{S,D} = m_{S,R_j} = m_{R_j,D} = 2$, $\bar{h}^2_{S,D} = 1$.

The best BER performance for the considered system is depicted in **Figure 11** when $m_{S,D}=m_{S,R_j}=m_{R_j,D}=2$, $\bar{h}^2_{S,D}=1$, and $M = 1$. It is seen that, for a fixed E_s/N_0, the performance of the considered system increases while $\in$ increases.

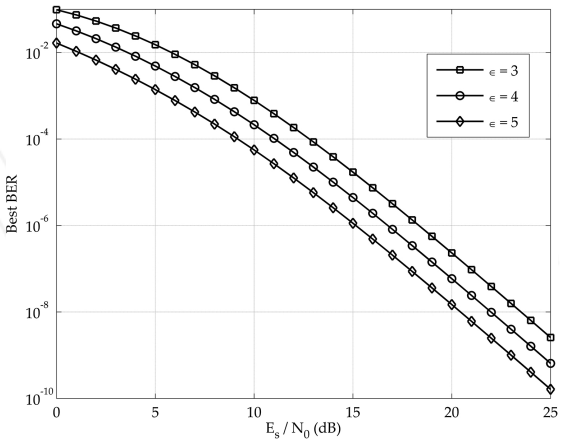

Figure 11. BER performance of the DF scheme for the cooperative-diversity relay network with $\in$ = 3, 4, 5 and $m_{S,D}=m_{S,R_j}=m_{R_j,D}=2$.

The variation of the optimal $d_{S,R}$ with varying E_s/N_0 for different values of $\in$ is depicted in **Figure 12**. We assume $m_{S,D}=m_{S,R_j}=m_{R_j,D}=2$, and $\bar{h}^2_{S,D}=1$.

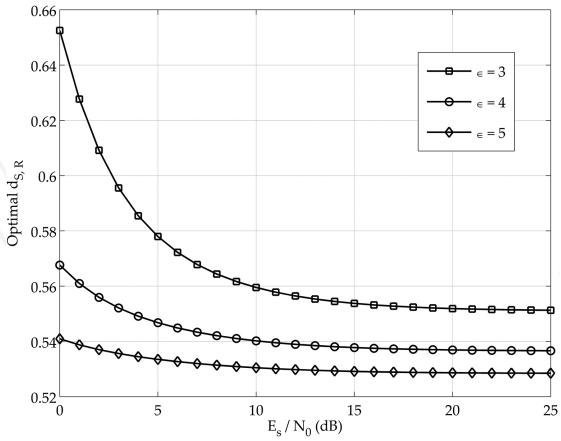

Figure 12. Optimal $d_{S,R}$ against different E_s/N_0 values with $\in$ = 3, 4, 5 and $m_{S,D}=m_{S,R_j}=m_{R_j,D}=2$.

Finally, the ROC (receiver operating characteristics) curves for $\in = 4$ are depicted in **Figure 13**. The fading parameters are set to be $m_{S,D}=m_{S,R_j}=m_{R_j,D}=1$, $m_{S,D}=m_{S,R_j}=m_{R_j,D}=2$, and $m_{S,D}=m_{S,R_j}=m_{R_j,D}=3$ successively. It can be observed from the figure that the best BER decreases with the fading parameters for a fixed value of E_s/N_0.

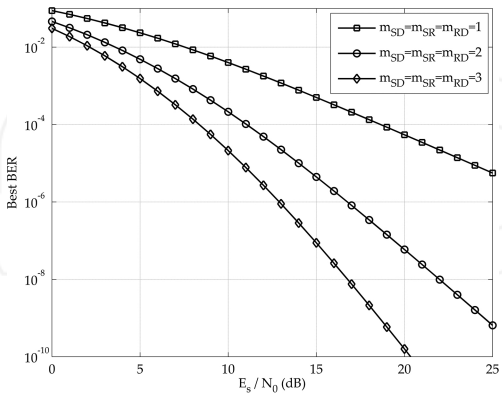

Figure 13. Error probability of DF scheme for the cooperative-diversity relay network using different fading parameter values with $\left(m_{S,D}=m_{S,R_j}=m_{R_j,D}\right)=1,\ 2,\ 3$.

4. Conclusions

In this paper, we present a comprehensive performance comparison of the DE and PSO algorithms both in FSO and in mobile radio communications systems. For the first part, we investigate the optimal transmission distances for different number of relay nodes and power margin values in the parallel DF relaying scheme. Moreover, we analyze the cost function and the execution time for the DE and PSO algorithms. As a second part of this paper, we consider the cooperative-diversity relay network for the mobile radio communications systems operating over Nakagami-m fading channel. We provide a rigorous data for the optimal locations of the relaying terminal in the parallel DF relaying scheme using DE and PSO algorithms. Then, we analyze the bit error probability with varying E_s/N_0 using different values of path loss exponent, $\in$ and fading parameters of $m_{S,D}$, m_{S,R_j}, and $m_{R_j,D}$.

We demonstrate that the cost functions are suitably minimized proving the accuracy of the employed optimization algorithms. We find out that both algorithms have similar execution time, besides PSO is more stable than the DE algorithm. Furthermore, the PSO algorithm outperforms DE algorithm with regard to the cost function. It should be emphasized that both optimization algorithms are reliable and can be used for the applications both in the FSO and mobile radio communications systems.

Author details

Arif Basgumus[1*], Mustafa Namdar[1], Gunes Yilmaz[2] and Ahmet Altuncu[1]

*Address all correspondence to: arif.basgumus@dpu.edu.tr

1 Dumlupinar University, Department of Electrical and Electronics Engineering, Kutahya, Turkey

2 Uludag University, Department of Electrical and Electronics Engineering, Bursa, Turkey

References

[1] Knievel C, Hoeher PA. On particle swarm optimization for MIMO channel estimation. J. Electr. Comput. Eng. 2011;2012:1–10. doi:10.1155/2012/614384.

[2] Su L, Wang P, Liu F. Particle swarm optimization based resource block allocation algorithm for downlink LTE systems. In: IEEE Asia-Pacific Conference on Communications (APCC '12); 15–17 October 2012; Jeju Island, IEEE; 2012. pp. 970–974.

[3] Dunand FR, Abrao T. Energy-efficient power allocation for WDM/OCDM networks with particle swarm optimization. J. Opt. Commun. Netw. 2013;5:512–523. doi:10.1364/JOCN.5.000512.

[4] Manickavelu D, Vaidyanathan RU. Particle swarm optimization (PSO)-based node and link lifetime prediction algorithm for route recovery in MANET. EUROSIP J. Wirel. Commun. Netw. 2014;2014:1–10. doi:10.1186/1687-1499-2014-107.

[5] Omidvar A, Mohammadi K. Particle swarm optimization in intelligent routing of delay-tolerant network routing. EUROSIP J. Wirel. Commun. Netw. 2014;2014:1–8. doi:10.1186/1687-1499-2014-147.

[6] Xiang L, Ximing L, Ercan MF, Yi Z. A new hybrid algorithm based on collaborative line search and particle swarm optimization. In: IEEE International Conference on Autonomous Robots and Agents (ICARA '09); 10–12 February 2009; Wellington, IEEE; 2009. pp. 486–489.

[7] Namdar M, Ilhan H, Durak-Ata L. Dispersed chirp-z transform-based spectrum sensing and utilization in cognitive radio networks. IET Signal Process. 2014;8:320–329. doi:10.1049/iet-spr.2013.0127.

[8] Namdar M, Ilhan H, Durak-Ata L. Partial spectrum utilization for energy detection in cognitive radio networks. In: IEEE International Congress on Ultra Modern Telecommunications and Control Systems (ICUMT '12); 3–5 October 2012; St. Petersburg, IEEE; 2012. pp. 989–994.

[9] Safari M, Uysal M. Relay-assisted free-space optical communication. IEEE Trans. Wirel. Commun. 2008;7:5441–5449. doi: 10.1109/T-WC.2008.071352.

[10] Karimi M, Nasiri-Kenari M. Free space optical communications via optical amplify-and-forward relaying. J. Lightwave Technol. 2011;29:242–248. doi:10.1109/JLT.2010.2102003.

[11] Karimi M, Nasiri-Kenari M. BER analysis of cooperative systems in free-space optical networks. J. Lightwave Technol. 2009;27:5639–5647. doi:10.1109/JLT.2009.2032789.

[12] Karimi M, Nasiri-Kenari M. Outage analysis of relay-assisted free space optical communications. IET Commun. 2010;4:1423–1432. doi:10.1049/iet-com.2009.0335.

[13] Kashani MA, Uysal M. Outage performance and diversity gain analysis of free-space optical multi-hop parallel relaying. J. Opt. Commun. Netw. 2013;5:901–909. doi: 10.1364/JOCN.5.000901.

[14] Kashani MA, Safari M, Uysal M. Optimal relay placement and diversity analysis of relay-assisted free-space optical communications systems. J. Opt. Commun. Netw. 2013;5:37–47. doi:10.1364/JOCN.5.000037.

[15] Ikki SS, Ahmed MH. Performance of cooperative diversity using equal gain combining (EGC) over Nakagami-m fading channels. IEEE Trans. Wirel. Commun. 2009;8:557–562. doi:10.1109/TWC.2009.070966.

[16] Namdar M, Sahin B, Ilhan H, Durak-Ata L. Chirp-z transform based spectrum sensing via energy detection. In: IEEE Signal Processing and Communications Applications Conference (SIU '12); 18–20 April 2012; Mugla, IEEE; 2012. pp. 1–4

[17] Ikki SS, Ahmed MH. Performance analysis of decode-and-forward cooperative diversity using differential EGC over Nakagami-m fading channels. In: IEEE Vehicular Technology Conference (VTC '09); 26–29 April 2009; Barcelona, IEEE; 2009. pp. 1–6.

[18] Ikki SS, Ahmed MH. Performance of multiple-relay cooperative diversity systems with best relay selection over Rayleigh fading channels. EURASIP J. Adv. Signal Process. 2008;2008:1–7. doi:10.1155/2008/580368.

[19] Ikki SS, Ahmed MH. Performance analysis of cooperative diversity using equal gain combining (EGC) technique over Rayleigh fading channels. In: IEEE International Conference on Communications (ICC '07); 24–28 June 2007; Glasgow, IEEE, 2007. pp. 5336–5341.

[20] Namdar M, Ilhan H, Durak-Ata L. Optimal detection thresholds in spectrum sensing with receiver diversity. Wirel. Personal Commun. 2016;87:63–81. doi:10.1007/s11277-015-3026-6.

[21] Olabiyi O, Annamalai A. Analysis of cooperative relay-based energy detection of unknown deterministic signals in cognitive radio networks. In: The International Conference on Wireless Networks (ICWN '11); 18–21 July 2011; Nevada. pp. 1–6.

[22] Atapattu S, Tellambura C, Jiang H. Relay based cooperative spectrum sensing in cognitive radio networks. In: IEEE Global Telecommunications Conference (GLOBECOM '09); 30 November–4 December 2009; Honolulu, IEEE, 2009. pp. 1–5.

[23] Atapattu S, Tellambura C, Jiang H. Energy detection based cooperative spectrum sensing in cognitive radio networks. IEEE Trans. Wirel. Commun. 2011;10:1232–1241. doi:10.1109/TWC.2011.012411.100611.

[24] Waqar OD, McLernon C, Ghogho M. Performance analysis of non-regenerative opportunistic relaying in Nakagami-m fading. In: IEEE International Symposium on Personal, Indoor and Mobile Radio Communications (PIMRC '09); 13–16 September 2009; Tokyo, IEEE; 2009. pp. 231–235.

[25] Waqar OD Mughal MO, Gu J, Kim JM. Detection probability analysis for AF assisted cooperative spectrum sensing in cognitive radio networks. In: IEEE International Conference on ICT Convergence (ICTC '11); 28–30 September 2011, Seoul, IEEE; 2011. pp. 461–464.

[26] Mughal MO, Razi A, Kim JM. Tight upper bounds on average detection probability in cooperative relay networks with selection combiner. Trans. Emerg. Telecommun. Technol. 2013;25:340–345. doi:10.1002/ett.2649.

[27] Basgumus A, Namdar M, Yilmaz G, Altuncu A. Performance comparison of the differential evolution and particle swarm optimization algorithms for the parallel DF relaying in free-space optical communications systems. Adv. Electr. Comput. Eng. 2015;15:17–22. doi:10.4316/AECE.2015.02003.

[28] Namdar M, Ilhan H, Durak-Ata L. Spectrum sensing for cognitive radio with selection combining receiver antenna diversity. In: IEEE Signal Processing and Communications Applications Conference (SIU '13); 24–26 April 2013; Haspolat, IEEE; 2013. pp. 1–4.

[29] Laneman JN, Tse DNC, Wornell GW. Cooperative diversity in wireless networks: efficient protocols and outage behaviour. IEEE Trans. Inform. Theor. 2004;50:3062–3080. doi:10.1109/TIT.2004.838089.

[30] Laneman JN, Wornell GW. Distributed space-time coded protocols for exploiting cooperative diversity in wireless networks. IEEE Trans. Inform. Theor. 2003;49:2415–2525. doi:10.1109/TIT.2003.817829.

[31] Avestimehr AS, Tse DNC. Outage-optimal relaying in the low SNR regime. In: IEEE International Symposium on Information Theory (ISIT '05); 4–9 September 2005; Adelaide, IEEE; 2005. pp. 941–945.

INTECH

INTECH